

A NOVEL METHOD OF ELIMINATION OF LIGHT POLARIZATION CROSS SENSITIVITY ON TILTED FIBER BRAGG GRATING BENDING SENSOR

Damian Harasim, Sławomir Ciężczyk

Lublin University of Technology, Electrical and Information Technology Department, Nadbystrzycka Str. 36D, Lublin, Poland (✉ d.harasim@pollub.pl, +48 81 538 4313, s.ciezczyk@pollub.pl)

Abstract

The article shows the possibility of using TFBG gratings to measure the radius of curvature of fiber bending in conditions of variable polarization of the introduced light. Most of the modern, stable light sources generate light with a high degree of polarization. Due to the spatial asymmetry, the direction of the light polarization plane affects the spectral parameters of individual modes. For this reason, in the measurement systems using TFBGs presented so far it becomes necessary to determine and control the state of light polarization directly in front of the periodic structure. The article presents the determined spectral parameters of the cladding modes which allow bending measurements regardless of the direction of polarization of the introduced light. Thanks to this, the measuring system can be constructed without providing control of the introduced light polarization angle, which makes its construction simpler. When using TFBGs with an angle of 2° , the accuracy of determining the bending radius in the range from 15 mm to 30 mm when changing the angle of the plane of polarization in the full range is 0.318 mm in the case of changes in the transmission coefficient. For changes in the wavelength of the selected cladding mode, the accuracy is 0.3203 mm, with the input light polarization being changed in the range from 0° (P type) to 90° (S type).

Keywords: tilted Bragg grating, optical fiber sensor, polarization, bending measurement.

© 2022 Polish Academy of Sciences. All rights reserved

1. Introduction

Sensors based on periodic fiber structures are still in great demand due to a number of advantages over traditional electronic ones. The most commonly used are conventional *fiber Bragg gratings* (FBG) which are inscribed by the creation of series of periodic zones with a raised refractive index in the fiber core. Their ability to reflect radiation with a particular wavelength is used in temperature and strain measurements [1–3]. Except for the very small size of the transducer and immunity to electromagnetic interference, they stand out with great multiplexing ability for inscription in a single optical fiber [4]. In the case of FBGs, the spectral parameters of such structures are affected only by quantities which change properties of light transmission in the core. One of the possible modification of the internal structure of a grating is introducing some tilt

between the planes of refractive index modulations and the cross-section plane of the optical fiber, which allows to create *tilted fiber Bragg gratings* (TFBGs) [5–7]. In such structures, some of the light transmitted through the fiber core is transferred into the cladding which can be observed in the spectrum as a series of transmission dips related to the following resonances with decreasing wavelengths. Transmission through the fiber cladding makes its spectral parameters dependent on the conditions related to changes in the cladding parameters. As a result, structures of this kind are most often used in measurements of the refractive index [8, 9]. Coating optical fiber in the section with a TFBG with a thin metallic (usually gold) layer leads to obtaining *Surface Plasmon Resonance* (SPR). The wavelength shift of selected resonances related to SPR is used for example in detection of biomarkers [10, 11]. They are based on the interaction between the *surrounding refractive index* (SRI) and the evanescent field of light propagating inside special fibers or fiber devices, such as cladding-etched fibers, side-polished fibers or *long-period gratings* (LPGs) [12]. The spectral parameters of resonances coupled by LPGs are also sensitive to changes of fiber stress caused by *e.g.* bending of fiber [13].

In the case of TFBGs, the intrinsic sensitivities, instead of SRI, include the input light polarization angle and the curvature of the fiber in the section with inscribed grating. Dependency on polarization is most commonly used for measurements of the twist of rotation between two points [14]. Such a measurement system needs to affect the mutual angle between input light polarization and the internal structure of the TFBG [15, 16]. In the case of bending, it is also reported that changes of fiber curvature affect spectral parameters of some cladding modes due to additional stress caused by the compressing or extending sections of the fiber cross-section [17, 18].

This paper presents an analysis of the influence of input light polarization on the spectral parameters related to the bending radius of the TFBG with the 2° tilt angle of internal structure. Most commonly used light sources generate strongly polarized light and in the usually presented measurements with TFBGs there is a need to control the polarization before the periodic transducer. It causes a complication in constructing of a measurement setup and could be a source of inaccuracies. In this paper it is argued that a TFBG with a certain tilt angle can operate as a bending transducer in selected curvature ranges independently of the input light polarization angle.

2. The principles of TFBG sensing properties

The main difference between TFBGs and conventional gratings is that in the case of tilted structures light transmitted by the fiber core is coupled into a series of cladding modes. These resonances could be observed in a transmission spectrum as a series of transmission loss peaks appearing at wavelengths lower than the Bragg wavelength.

The Bragg wavelength, corresponding to the core mode, is given by:

$$\lambda_B = \frac{2n_{\text{eff}}^{\text{core}}}{\cos \Theta} \Lambda, \quad (1)$$

where $n_{\text{eff}}^{\text{core}}$ is the effective refractive index of the core, Λ is the period of grating and Θ is the angle of the internal structure tilt. Figure 1 presents a side view of an optical fiber with periodic zones of a greater refractive index inscribed with tilt angle Θ_{TFBG} .

Periodic zones of refractive index perturbations inscribed with a particular tilt are the reason why the light is transferred from the core mode into a series of cladding resonances. The wavelengths of the cladding modes, related to the backwards-propagating coupling between the

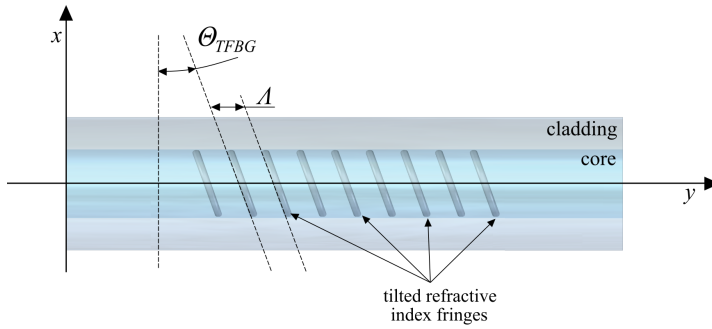


Fig. 1. Schematic view of an optical fiber side with refractive index perturbations inscribed at an Θ_{TFBG} angle.

cladding modes and the core mode, are given by the following formula:

$$\lambda_k^{\text{clad}} = \frac{n_{\text{eff}}^{\text{core}} + n_{\text{eff}_k}^{\text{clad}}}{\cos \Theta} \Lambda, \quad (2)$$

where $n_{\text{eff_clad}}$ is the effective refractive index of the i -th cladding mode, $i = 1 \dots m$, where m is the total number of cladding modes. The reflectivity of individual resonant modes $R_i^{\text{co,cl}}$ depends on the modulation of the refractive index as in the following expression [19]:

$$R_i^{\text{co,cl}} = \tanh^2 \left\{ LC \iint_{-\infty}^{+\infty} \vec{E}^{\text{co}} \times \vec{E}^{\text{cl}} \Delta n \cos \left(\frac{4\pi}{\Lambda} z \cos(\theta_{TFBG}) + y \sin(\theta_{TFBG}) \right) dx dy \right\}, \quad (3)$$

where L is the length of the grating, C is a proportional constant related to the normalisation of the transverse mode fields, and Δn is the function describing the variation of the refractive index due to the grating cross-section in the fiber.

A decrease in fiber curvature (an increase in bending) induces a longitudinal strain ε which is oriented parallel to the optical axis, where $\varepsilon = C_y$ and C is the bending curvature defined as the inverse of the bending radius R . Parameter y is related to the distance. According to the photoelastic effect, the introduced strain creates a refractive index change Δn expressed as [20]:

$$\Delta n = - \left(\frac{n^3}{2} \right) [(1 - \nu)p_{12} - \nu p_{11}] C_y, \quad (4)$$

where n is the refractive index, ν is the Poisson ratio, p_{11} and p_{12} are photoelastic constants.

2.1. Bending of fiber with a TFBG inscribed

Strain induced by bending the fiber results in a linear gradient of the refractive index in the bending plane. It has also been reported that the direction of bending according to the orientation of the tilted refractive index perturbations has an influence on the behavior of selected modes of spectral properties [21]. In the study presented in this paper, the orientation between the structure of the tilted fringes and the direction of the bending plane was maintained as presented in Fig. 2.

The bending plane applied in the experiments described in the next sections of the paper is presented schematically in Fig. 2. The plane was kept with the direction identical to the P-oriented polarization plane of input light. The markings characteristic of polarization angles will be described in the next subsection.

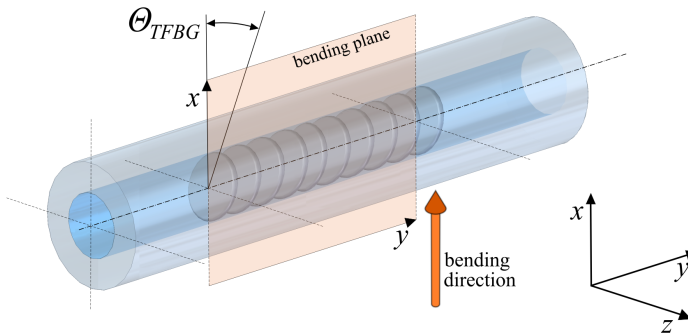


Fig. 2. Scheme of optical fiber with a TFBG inscribed and bending direction according to internal orientation of tilted periodic refractive index perturbations.

Figure 3. shows changes of spectral characteristics in the range of 1560–1565 nm for three selected values of the bending radius of the fiber with the produced TFBG: 15, 22.5 and 30 mm. It can be seen that with the contraction of the radius the wavelengths and the transmission coefficients of the cladding modes propagating in the immediate vicinity of the optical fiber core change. For a detailed analysis, the first LP_{11} mode was selected, which can be done from outside the minimum ghost mode. The wavelength of the LP_{11} cladding mode is monotonically shifted towards longer wavelengths. At the same time, a change in the amplitude of this resonance can be observed, manifested by an increase in the transmission coefficient.

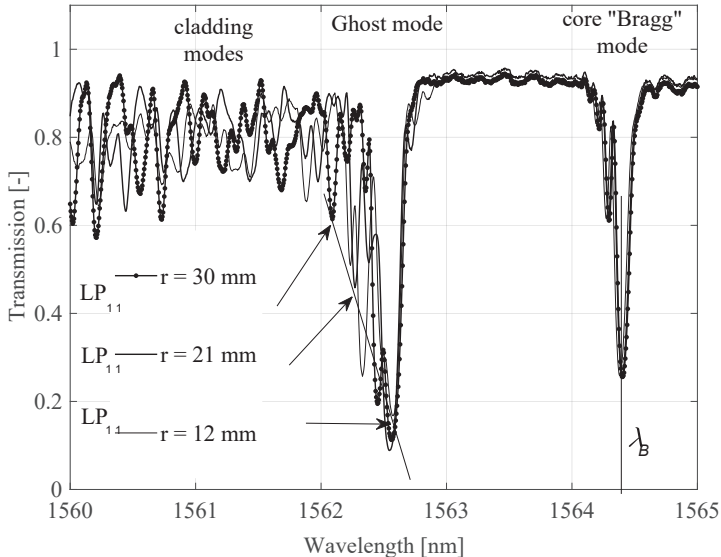


Fig. 3. Influence of changes in the bending radius on the spectral characteristics of a TFBG with an angle of 2° , measured in the wavelength range including the Bragg, ghost and lowest order cladding modes.

In addition, it can be observed that the part of the characteristics related to the occurrence of the core resonance (Bragg) is neither shifted nor changed in amplitude. The Bragg wavelength of the core mode can be used as a reference value for compensating for the temperature effect

on the characteristics. Changes in the ambient temperature cause a uniform shift of the entire spectrum of the TFBG structure. For this reason, the wavelength difference between the Bragg resonance and the cladding mode selected for analysis remains constant regardless of the ambient temperature.

2.2. Rotation of input light polarization angle

In the case of gratings with tilted planes of the refractive index perturbations, due to spatial asymmetry it is necessary to control the polarization angle in relation to the arrangement of the internal structure of the TFBG grating. In Fig. 4, two particular orientations of the plane of polarization of the input light in relation to the alignment of the interference fringes produced in the grating core are shown. The P-type polarization in the analyzed case means light polarized in the direction of the xy plane. The S-type polarization is related to the case perpendicular to the P-type. The marked angle Θ_{TFBG} is determined in the xy plane perpendicular to the plane of the cross-section of the fiber.

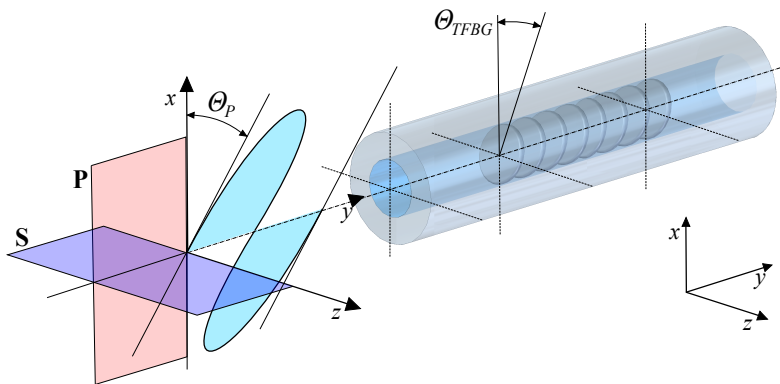


Fig. 4. Illustration of introducing linearly polarized light into the TFBG structure with characteristic P-type and S-type polarization angles.

Determining appropriate spectral parameters, subject to monotonic change with the change of the light polarization angle, allows to measure the rotation angle between selected points in the structure. The measurement method based on determining changes in the transmission coefficient for a selected wavelength is called the spectral line method. The use of such analysis requires the determination of one wavelength, for which the changes of the transmission coefficient will remain monotonic along with the changes of the measured quantity. The wavelength which could be used in such analysis of single cladding mode transmission is presented in Fig. 6. In this case, for 1547.15 nm the transmission is monotonically changing with rotation of input light polarization from P-state to S-state. Figure 6 shows the spectrum of the LP_{016} cladding mode selected for the analysis in a narrow spectral range.

Figure 5 shows changes in the shape of the spectrum of the selected cladding mode with three characteristic angles of polarization of the input light. There is a characteristic separation into two distinguishable resonances: characterized by a shorter central wavelength, the so-called odd mode and the so-called even mode. Additionally, the wavelengths of both resonances of 1547.09 nm and 1547.15 nm were determined for which the analysis of changes in the transmission coefficient for changes in the polarization angle of the light introduced into the fiber was carried out.

The dependence of the amplitude value for the selected wavelength on the polarization angle of the radiation entering the fiber is shown in Fig. 6.

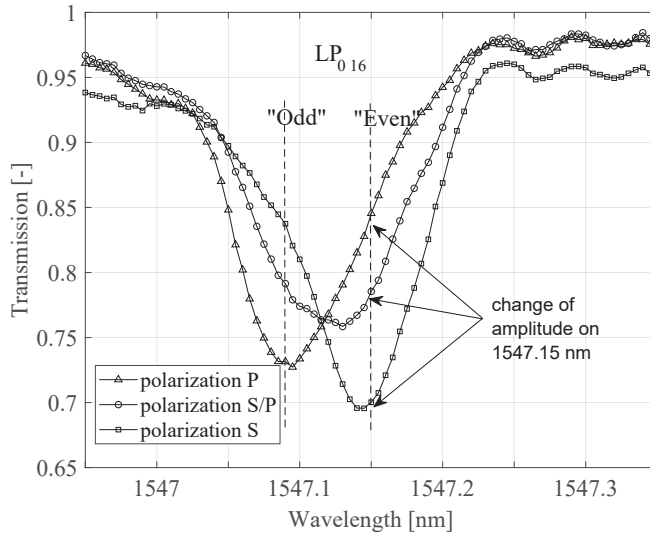


Fig. 5. Transmission spectra of the TFBG 2° grating measured for 3 characteristic polarizations of the input light.

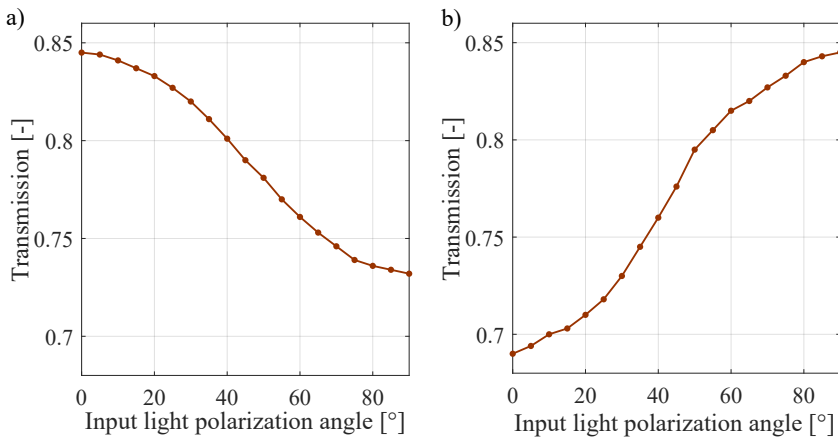


Fig. 6. Characteristics of the transmission coefficient of the LP₀₁₆ cladding mode separated into two resonances: a) odd mode, b) even mode.

The polarization angles of the introduced light constituting the horizontal axis in Fig. 6 refer to the Θ_P angle marked in Fig. 3 where the value of 0° corresponds to the P-type polarization and the value of 90° indicates the S-type state. On their basis, the results indicate that the highest order modes show high sensitivity to changes in the angle of rotation of the polarization of the introduced light. At the same time, modes with wavelengths close to the ghost mode are relatively independent of the polarization state.

3. Measurement of bending with variable input light polarization angle

This section presents the effect of changes in the polarization angle of the light introduced on the spectral characteristics of TFBG parameters with an angle of 2° related to the bending radius of the fiber. The measuring system made it possible to set the polarization angle of the introduced light and to change the bending radius of the optical fiber in the place with the TFBG grating inscribed. Stable fastening of the fiber between the plates protects against the effect of twisting or rotating of the fiber. During the measurements, the fiber was positioned in such a way that the internal structure of the TFBG was positioned in relation to the bending plane as shown in Fig. 2.

The scheme of the measurement system is presented in Fig. 7. The polarizer installed in it ensures a high degree of linear light polarization. A half-wave plate was used for rotation of the input light polarization angle. The TFBG used in the conducted experiments was inscribed by using the phase mask method with an excimer KrF laser. The optical fiber was THORLABS GF1 photosensitive fiber with a Ge dope.

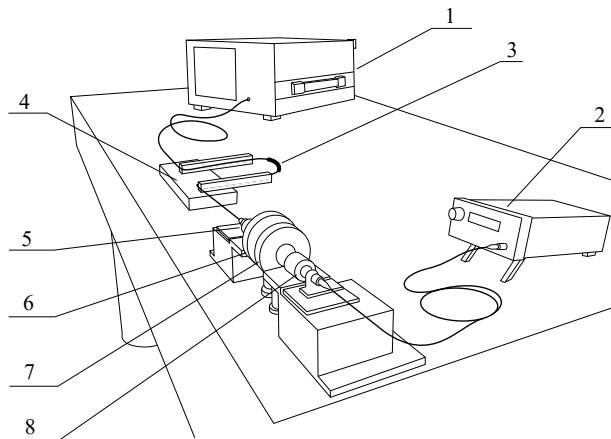


Fig. 7. Scheme of the measurement system. 1 – Yokogawa AQ630D optical spectrum analyzer (OSA), 2 – THORLABS S5FC1005S broadband SLED source, 3 – TFBG with a 2° internal angle, 4 – translation stage for adjustment of fiber bending, 5, 8 – objectives, 6 – half-wave plate, and 7 – a polarizer.

The first analyzed case was the determination of influence of changes in the polarization angle of light introduced into the optical fiber on the spectral parameters, proving the changes in the bending radius of the fiber with a tilted Bragg grating. The spectral parameters, *i.e.* the transmission coefficient and the wavelength of the LP_{11} mode, were analyzed. Figure 8 shows the spectral characteristics of selected spectral ranges of the low-order mode LP_{11} determined for three extreme cases of the polarization of the introduced light: state P, state S and the transient P/S, as well as for two bending radii: 30 mm (a) and 15 mm (b). In the case of the polarization angles of light changing between extreme states, *i.e.* from $\Theta_P = 0^\circ$ (P) to $\Theta_P = 90^\circ$ (S), the changes in spectral parameters are monotonic. Therefore, it should be assumed that the potential impact of polarization changes on the parameters related to the determination of the bending radius will be the most significant just for the extreme cases.

The characteristics presented in Fig. 8 clearly show that with changes in the polarization angle of the light introduced into the TFBG structure, the spectra of the low-order cladding modes within 1560–1563 nm wavelength range do not change significantly. Cladding modes with longest wavelengths present the highest sensitivity for bending. Figure 9 shows the characteristics of

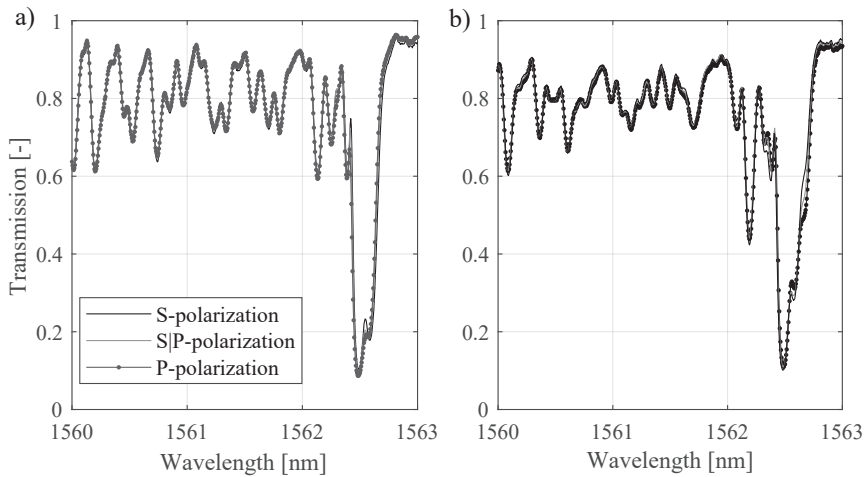


Fig. 8. Transmission spectra of 2° tilt grating measured for: a) bending radius of 30 mm and b) 20 mm at the angles of polarization of the introduced light S, S|P and P.

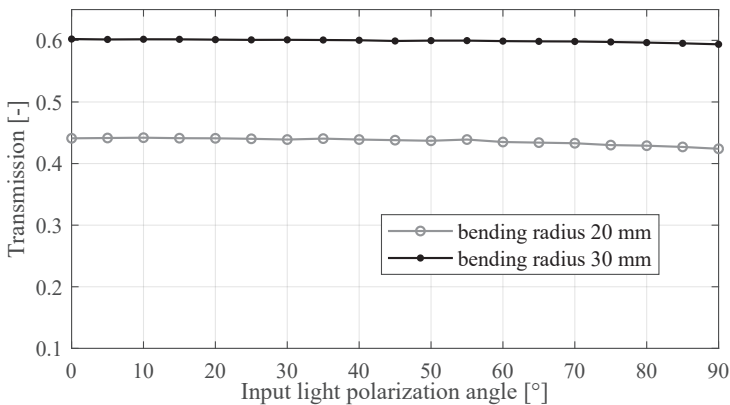


Fig. 9. Changes of the LP_{11} mode transmission coefficient.

changes in the LP_{11} mode transmission coefficient, determined for changes in the light polarization angle in the range of 0° to 90° (between P and S). The transmission coefficient values are presented in the range from 0.1 to 0.6, which reflects the range of changes in the LP_{11} mode transmission coefficient for changes in the bending radius in the assumed range from 15 mm to 30 mm. In addition to the low-order cladding mode transmission coefficient, the parameter dependent on the bending radius of the fiber is the minimum transmission wavelength for this mode. Considering this, the characteristic of changes in the central wavelength of the LP_{11} mode with changes in the bending radius was determined for the three extreme cases of the polarization of the introduced light: P, S and P/S type.

Figure 10a shows the characteristics of changes in the transmission coefficient to radius of fiber curvature, while Fig. 10b shows the changes in the central wavelength of the low-order mode determined for three extreme cases of the introduced light polarization: P state, S state and medium P/S.

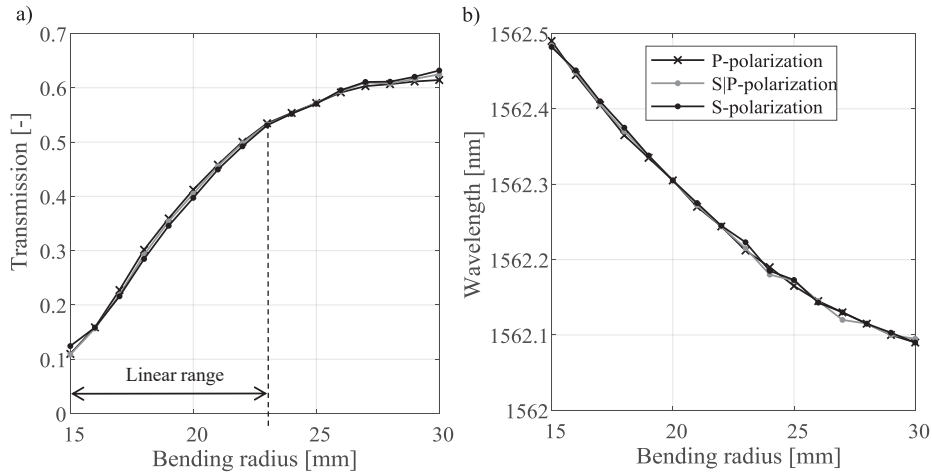


Fig. 10. Characteristics of the transmission coefficient (a) and the central wavelength (b) of the LP_{11} cladding mode to bending radius for three polarization cases.

The characteristics presented in Fig. 10 show that despite the introduction of light with extremely different polarization angles, the nature of changes in both the central wavelength and the transmission coefficient of the selected mode are preserved. The differences in the values of the parameters indicated above when changing the polarization are insignificant. Analysis of Fig. 10a shows that in the case of a bend with a radius of 15 mm to 23 mm, the characteristic of the coefficient related to the amplitude of the signal measured for the selected wavelength retains its shape close to linear.

The graphs in Fig. 10a are additionally given a straight line of linear approximation determined for averaged values of the transmission coefficient determined for successive fiber bending radii. Table 1 shows the values of the transmission coefficient determined for the LP_{11} mode when increasing the bending radius of the fiber at three polarization states of the introduced radiation. Within the assumed range of fiber curvature, the greatest difference between the transmission power values is 0.0169. Assuming that for the bending radii from 15 to 23 mm the change of the coefficient is 0.4241, this translates into the error of determining the bending radius equal to 0.318 mm.

Another spectral parameter related to the bending radius, the changes of which in the selected range maintain a shape close to linear, is the central wavelength of the selected LP_{11} cladding

Table 1. Values of the LP_{11} mode transmission coefficient determined for three cases of polarization and for several fiber bending radii.

Bending radius [mm]	Transmission of LP_{11} mode polarization P	Transmission of LP_{11} mode polarization P S	Transmission of LP_{11} mode polarization S	Biggest difference
15	0.1243	0.1087	0.1098	0.0156
17	0.2159	0.2187	0.2274	0.0028
19	0.3458	0.3541	0.3594	0.0136
21	0.4494	0.4556	0.4583	0.0089
23	0.5308	0.5328	0.5346	0.0038

mode. Figure 10b shows the characteristics of the LP₁₁ mode wavelength shift caused by the changes in the bending radius, determined on the basis of the spectra measured for the three previously described cases of light polarization. The graphs presented in Fig. 10b, as in the case of the transmission coefficient considered earlier, mean that the change of the light polarization angle does not significantly change the shape of the transition characteristics.

Table 2 presents a summary of the determined central wavelengths of the LP₁₁ mode with three characteristic cases of the input light polarization for the changing bending radius of the fiber with the TFBG structure recorded.

Table 2. Values of the central wavelength of the LP₁₁ mode determined for three cases of polarization and a variable bending radius of the fiber.

Bending radius [mm]	Center wavelength LP ₁₁ polarization P	Center wavelength LP ₁₁ polarization P S	Center wavelength LP ₁₁ polarization S	Biggest difference
15	1562.482	1562.484	1562.49	0.008
17	1562.41	1562.406	1562.405	0.005
19	1562.338	1562.338	1562.335	0.003
21	1562.275	1562.272	1562.27	0.005
23	1562.223	1562.215	1562.212	0.011

For the selected range of bending radii the change in the wavelength of the LP₁₁ mode is 0.309 nm. The greatest difference between the wavelengths presented in Table 2 is 0.011 nm which translates into an error in determining the bending radius related to the polarization state of the introduced light of 0.3203 mm.

Figure 11 shows the characteristics displaying the values of the largest difference between the values of the transmission coefficient (a) and the central wavelength of the mode (b) determined for the P, S and P/S polarization states.

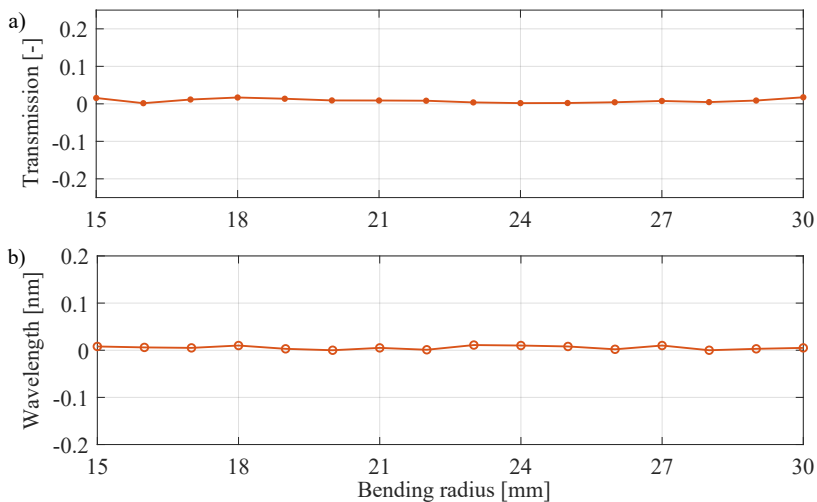


Fig. 11. Change of the value of the greatest difference between the values of: a) transmission coefficient; b) the central wavelength of the LP₁₁ mode determined for successive bending radii for three values of the input light polarization: S, P and S|P.

The shape of the characteristics shows that in the range of bending radii from 15 mm to 30 mm, the greatest differences in the transmission coefficient were noted for the extreme curvature values, which is consistent with Fig. 11. The central wavelength parameter maintains a constant value in the full assumed bending range.

4. Conclusions

This article presents the impact of changes in the polarization of light introduced into the TFBG structure on the spectral parameters of such a structure used to measure the bending radius. It was indicated that without polarization control, the measurement of the bending radius can be performed with a single TFBG with a 2° inclination angle in the range from 15 to 30 mm. The cladding modes and their spectral parameters were selected to be directly related to the value of the bending curvature of the fiber, which are, at the same time, independent of the light polarization angle. With regard to the ranges of changes in the transmission coefficient of the selected mode and the shift of its central wavelength, the uncertainties in determining the bending radius in the case of changes in the polarization of the input light in the full range, *i.e.* from the P-type polarization to the S-type state, were determined. In the case of measuring the transmission coefficient, the determination error is 0.318 mm, and in the case of measuring the shift of the central wavelength it is 0.3203 mm. This means that with limited accuracy, it is possible to measure the bending radius in the selected range without the need to control or determine the polarization angle of the introduced light.

Acknowledgements

This work was supported by the Lublin University of Technology grant number FD-20/EE-2/305.

References

- [1] Dziubiński, G., Harasim, D., Skorupski, K., Mussabekov, K., Kalizhanova, A., & Toigozhinova, A. (2016). Optimization of fiber optic sensors parameters for temperature measurement. *Rocznik Ochrona Środowiska*, 18(2), 309–324. https://ros.edu.pl/images/roczniki/2016/No2/23_ROS_N2_V18_R2016.pdf (in Polish)
- [2] Caucheteur, C., Guo, T., & Albert, J. (2017). Polarization-Assisted Fiber Bragg Grating Sensors: Tutorial and Review. *Journal of Lightwave Technology*, 35(16), 3311–3322. <https://doi.org/10.1109/JLT.2016.2585738>
- [3] Lo Presti, D., Massaroni, C., Jorge, C.S., Domingues, M.F., Sypabekova, M., Barrera, D., Floris, I., Massari, L., Oddo, C.M., & Sales, S. (2020). Fiber Bragg Gratings for Medical Applications and Future Challenges: A Review. *IEEE Access*, 8, 156863–156888. <https://doi.org/10.1109/ACCESS.2020.3019138>
- [4] Harasim, D., & Kisała, P. (2015). Interrogation systems for multiplexed fiber Bragg sensors. *Informatyka, Automatyka, Pomiary w Gospodarce i Ochronie Środowiska*, 4(5), 77–84. <https://doi.org/10.5604/20830157.1176580> (in Polish)
- [5] Guo, T., Liu, F., Guan, B.O., & Albert, J. (2016). Tilted fiber grating mechanical and biochemical sensors. *Optics & Laser Technology*, 78B, 19–33. <https://doi.org/10.1016/j.optlastec.2015.10.007>

- [6] Dong, X., Zhang, H., Liu, B., & Miao, Y. (2011). Tilted fiber Bragg gratings: Principle and sensing applications. *Photonic Sensors, 1*, 6–30. <https://doi.org/10.1007/s13320-010-0016-x>
- [7] Pilate, J., Renoirt, J.M., Caucheteur, C., Raquez, J.M., Meyer, F., Megret, P., Dubois, P., & Damman, P. (2014). Tilted fiber Bragg gratings as a new sensing device for in situ and real time monitoring of surface-initiated polymerization. *Polymer Chemistry, 5*(7), 2506–2512. <https://doi.org/10.1039/C3PY01421E>
- [8] Cieszczyk, S., Kisała, P., & Mrocza, J. (2019). New Parameters Extracted from Tilted Fiber Bragg Grating Spectra for the Determination of the Refractive Index and Cut-Off Wavelength. *Sensors, 9*(19), 1–11. <https://doi.org/10.3390/s19091964>
- [9] Cieszczyk, S., Harasim, D., & Kisała, P. (2017). A Novel Simple TFBG Spectrum Demodulation Method for RI Quantification. *IEEE Photonics Technology Letters, 24*(29), 2264–2267. <https://doi.org/10.1109/LPT.2017.2768601>
- [10] Duan, Y., Wang, F., Zhang, X., Liu, Q., Lu, M., Ji, W., Zhang, Y., Jing, Z., & Peng, W. (2021). TFBG-SPR DNA-Biosensor for Renewable Ultra-Trace Detection of Mercury Ions. *Journal of Lightwave Technology, 39*(12), 3903–3910. <https://opg.optica.org/jlt/abstract.cfm?URI=jlt-39-12-3903>
- [11] Wang, Q., Jing, J., & Wang, B. (2019). Highly Sensitive SPR Biosensor Based on Graphene Oxide and Staphylococcal Protein A Co-Modified TFBG for Human IgG Detection. *IEEE Transactions on Instrumentation and Measurement, 68*, 3350–3357. <https://doi.org/10.1109/TIM.2018.2875961>
- [12] Kim, D.W., Zhang, Y., Cooper, K.L., & Wang, A. (2005). In-fiber reflection mode interferometer based on a long-period grating for external refractive-index measurement. *Applied Optics, 44*(26), 5368–5373. <https://doi.org/10.1364/AO.44.005368>
- [13] Esposito, F., Sansone, L., Srivastava, A., Baldini, F., Campopiano, S., Chiavaioli, F., Giordano, M., Giannetti, A., & Iadicicco, A. (2020, October). Fiber optic biosensor for inflammatory markers based on long period grating. In 2020 Ieee Sensors (pp. 1–4). IEEE. <https://doi.org/10.1109/SENSOR47125.2020.9278773>
- [14] Harasim, D. (2017). The influence of fiber bending on polarization-dependent twist sensor based on tilted Bragg grating. *Metrology and Measurement Systems, 24*(3), 577–584. <https://doi.org/10.1515/mms-2017-0038>
- [15] Lu, Y., Shen, C., Chen, D., Chu, J., Wang, Q., & Dong, X. (2014). Highly sensitive twist sensor based on tilted fiber Bragg grating of polarization-dependent properties. *Optical Fiber Technology, 20*(5), 491–494. <https://doi.org/10.1016/j.yofte.2014.05.011>
- [16] Budinski, V., & Donlagic, D. (2017). Fiber-Optic Sensors for Measurements of Torsion, Twist and Rotation: A Review. *Sensors, 17*(3), 443. <https://doi.org/10.3390/s17030443>
- [17] Kisała, P., Skorupski, K., Cięższyk, S., Panas, P., & Klimek, J. (2018). Rotation and twist measurement using tilted fiber Bragg gratings, *Metrology and Measurement Systems, 25*(3), 429–440. <https://doi.org/10.24425/123893>
- [18] Feng, D., Zhou, W., Qiao, X., & Albert, J. (2015). Compact Optical Fiber 3D Shape Sensor Based on a Pair of Orthogonal Tilted Fiber Bragg Gratings. *Scientific Reports, 5*, 17415. <https://doi.org/10.1038/srep17415>
- [19] Albert, J., Shao, L.Y., & Caucheteur, C. (2013). Tilted fiber Bragg grating sensors. *Laser & Photonics Reviews, 7*(1), 83–108. <https://doi.org/10.1002/lpor.201100039>
- [20] Kisała, P., Mrocza, J., Cięższyk, S., Skorupski, K., & Panas, P. (2018). Twisted tilted fiber Bragg gratings: New structures and polarization properties. *Optics Letters, 43*, 4445–4448. <https://doi.org/10.1364/OL.43.004445>

- [21] Harasim, D. (2021). Temperature-insensitive bending measurement method using optical fiber sensors. *Sensors and Actuators A: Physical*, 332(2), 113207. <https://doi.org/10.1016/j.sna.2021.113207>



Damian Harasim received his M.Sc. degree in mechatronics from the Lublin University of Technology, Poland in 2014. He is currently working toward a Ph.D. degree in Automation, Electronics and Electrical Engineering at the Faculty of Electrical Engineering and Computer Science of this university. His current research interests are fabrication and characterisation of optical sensing systems, especially those based on unconventional Bragg structures.



Sławomir Ciężczyk is an associate professor at the Department of Electronics and Information Technology at the Lublin University of Technology. He received the Ph.D. degree in 2008 and the D.Sc. Degree (habilitation) in 2018. His research interests include optical sensors, open-path spectroscopy, signal processing, data analysis, numerical methods, simulation and modeling.